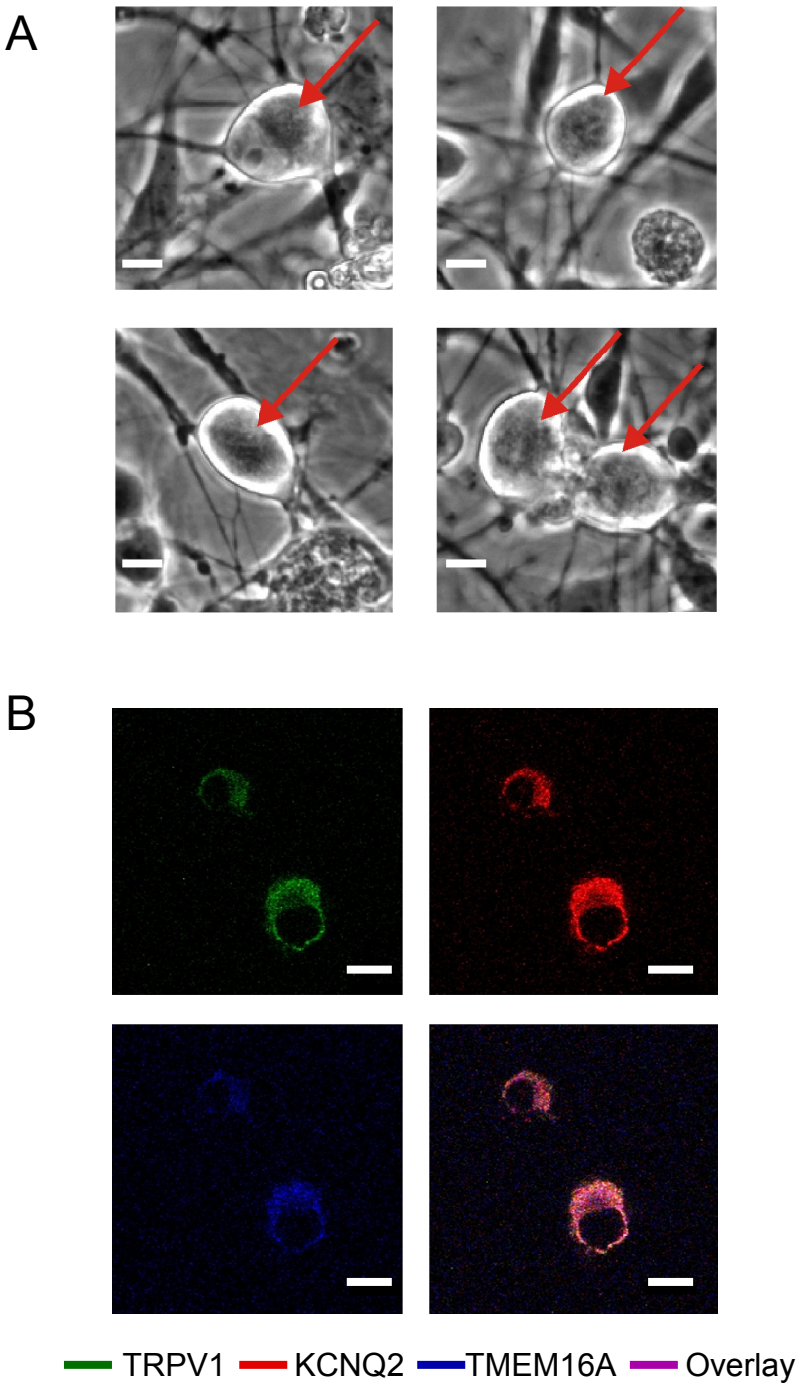

Supplementary Figure 1. (A) Phase contrast micrographs of the typical 'peanut-shaped' small DRG neurons in culture used for the patch-clamp recordings. (B) Co-expression of TRPV1, TMEM16A, and $K_v7.2$ in small DRD neurons. Scale bars are 5 μM in A and B. See Supplementary Methods for the staining details.

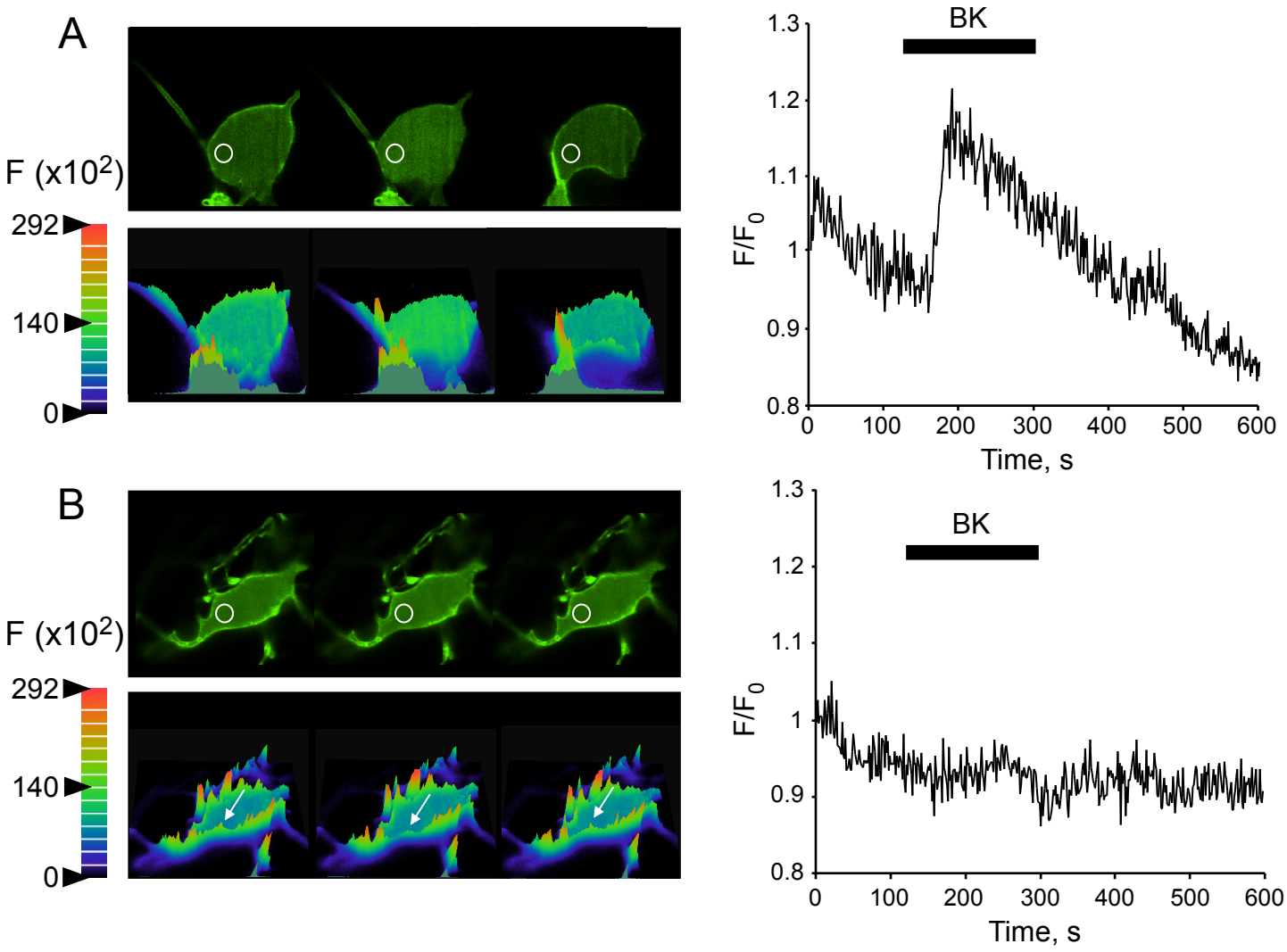

Supplementary Figure 2. Evaluation of BK-induced PIP_2 depletion in DRG neurons using YFP-tubby. Shown in (A) is the only YFP-tubby transfected DRG neuron (out of 12) which displayed measurable increase in cytosolic fluorescence following to BK application. Upper panel shows confocal micrographs of transfected DRG neuron before (left), during (middle) and after (right) application of 200 nM BK. Lower panel shows intensity surface plots for the images above. Plot on the right is normalised cytosolic fluorescence intensity measured within the area of interest indicated by the white circle. (B) depicts another neuron which show certain loss of fluorescence in one membrane patch (indicated by the white arrow), this however did not amount to any measurable changes in cytosolic fluorescence (as indicated by the fluorescence intensity plot on the right. All other conditions and labelling as in A.

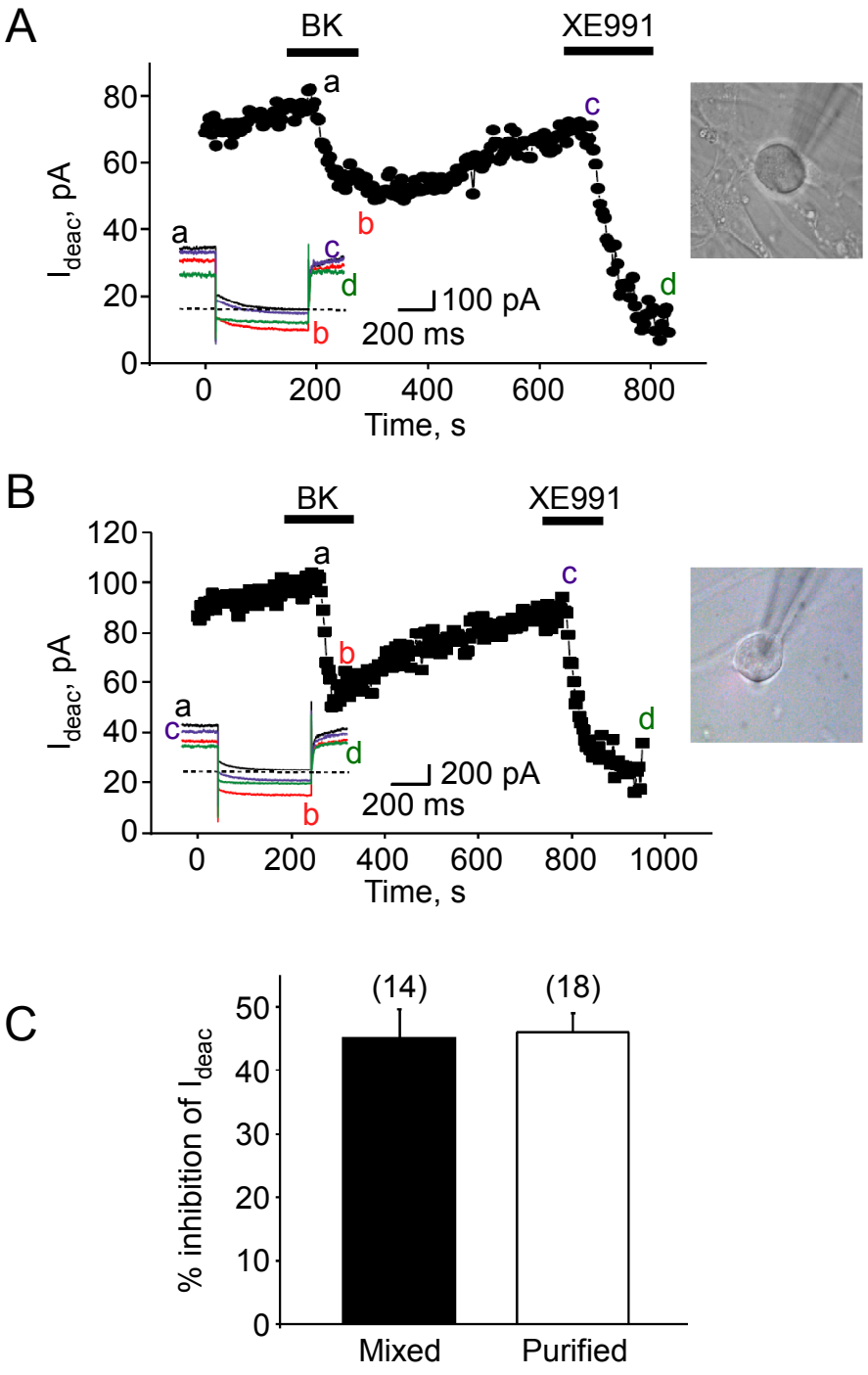

Supplementary Figure 3. The inhibitory effect of bradykinin on M current is independent of non-neuronal cells. DRG neurons were cultured under normal condition (A, 'mixed culture') or purified by replating and cytosine arabinoside treatment to eliminate non-neuronal cells (B, 'purified culture', see Supplementary Methods for the details). (A) - (B) Time course for the effect of bradykinin (200 nM) on M current cultured under either conditions. Current traces at different time points (indicated by the letters) are shown in the insets under the curves. The insets on the right show the phase-contrast photomicrograph of DRG neurons from which recordings have been made. (C) Summary of the bradykinin effect for two populations of DRG neurons.

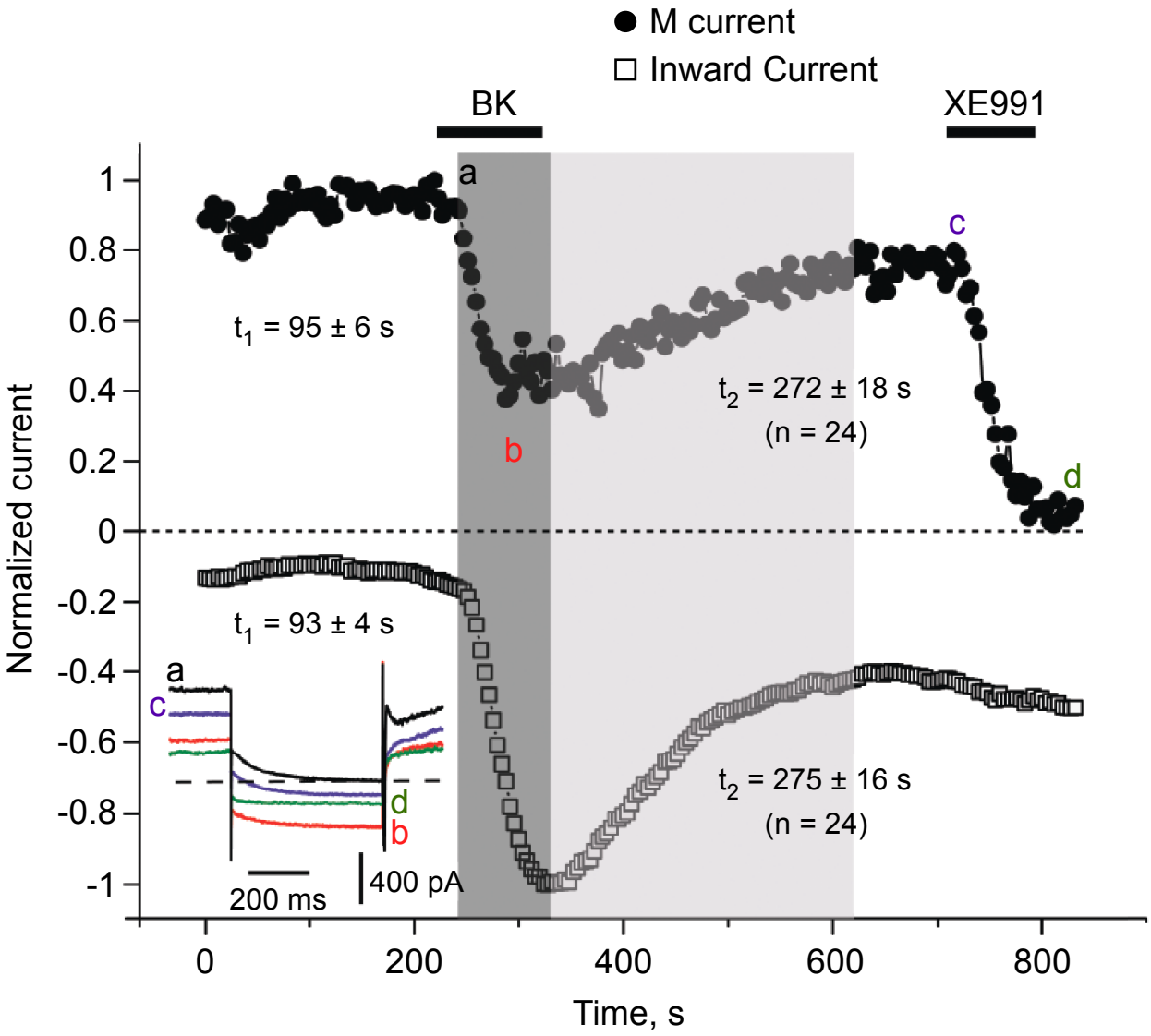

Supplementary Figure 4. Bradykinin-induced M current inhibition and inward current activation occur simultaneously. DRG neurons were voltage clamped under the protocol shown in Fig. 2A inset. M current was measured as the deactivating tail current at -60 mV and normalized to the basal level before BK application. Cl^- current was measured as the steady state current at -60 mV and normalized to its peak level. t_1 and t_2 represent the summary of the time for inhibition (M current) of activation (Cl^- current) and recovery/decay (M or Cl^- current respectively). Note that XE991 caused a complete inhibition of M current, however, it failed to induce an inward current.

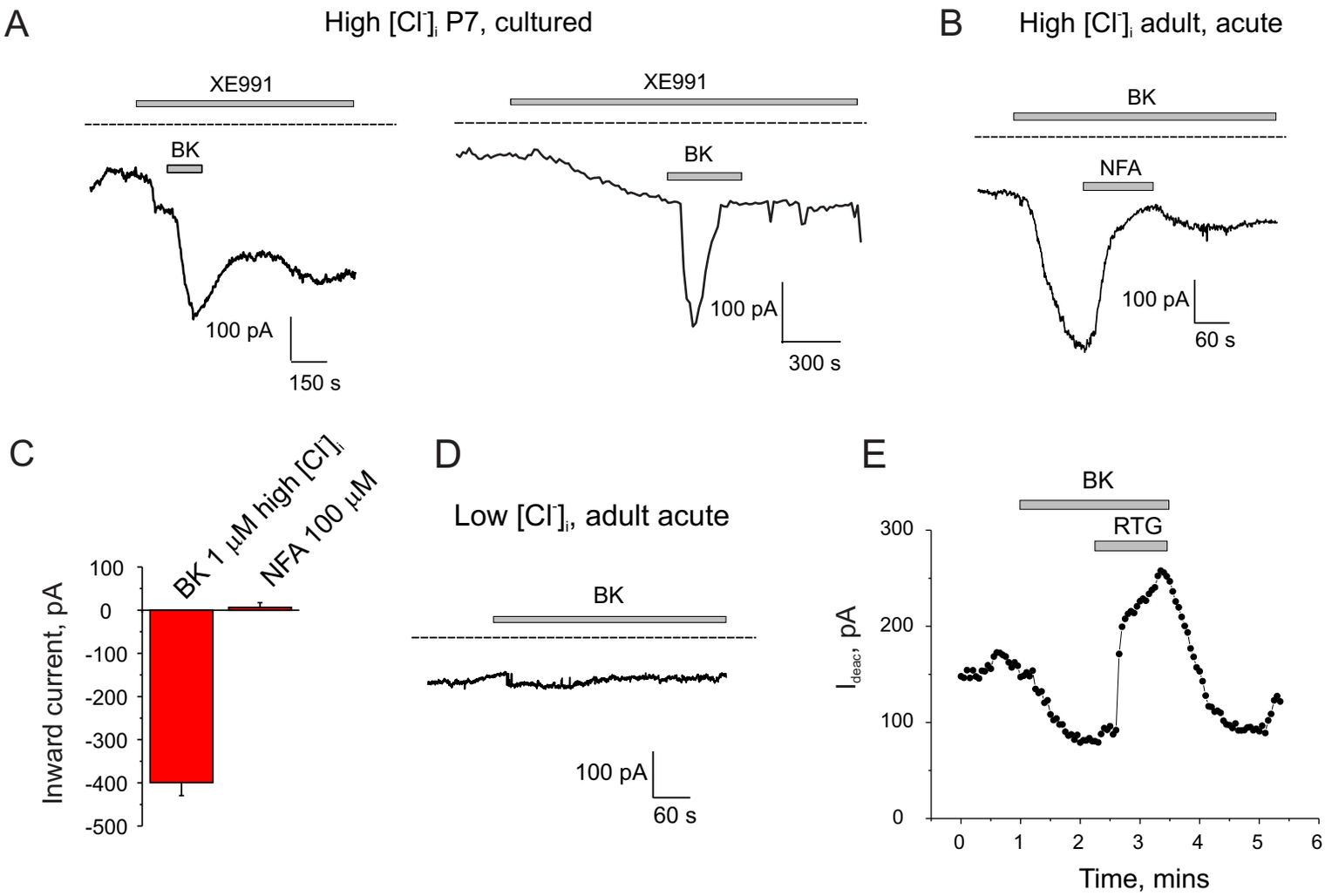

Supplementary Figure 5.(A) Perforated whole cell patch clamp recordings (amphotericin B with high intracellular chloride) on cultured DRGs from P7 rats. BK (200 nM) produced robust activation of an inward current at -60 mV in the presence of the M channel inhibitor XE991 (3 μM). Dotted line indicates zero current. (B) Amphotericin perforated whole cell recording from acutely dissociated adult rat DRG. BK (1 μM) produced a prominent inward current which was inhibited by niflumic acid (NFA, 100 μM). (C) Mean steady state currents using the protocol shown in B (BK, n = 8; NFA, n = 6). (D) Equivalent experiment to that shown in B but with low chloride in the pipette solution. (E) Whole cell amphotericin perforated recoding from DRG extracted from P7 rat then cultured for 2-5 days. M current inhibition by BK (1 μM) could be effectively reversed by bath application of retigabine (RTG, 10 μM)

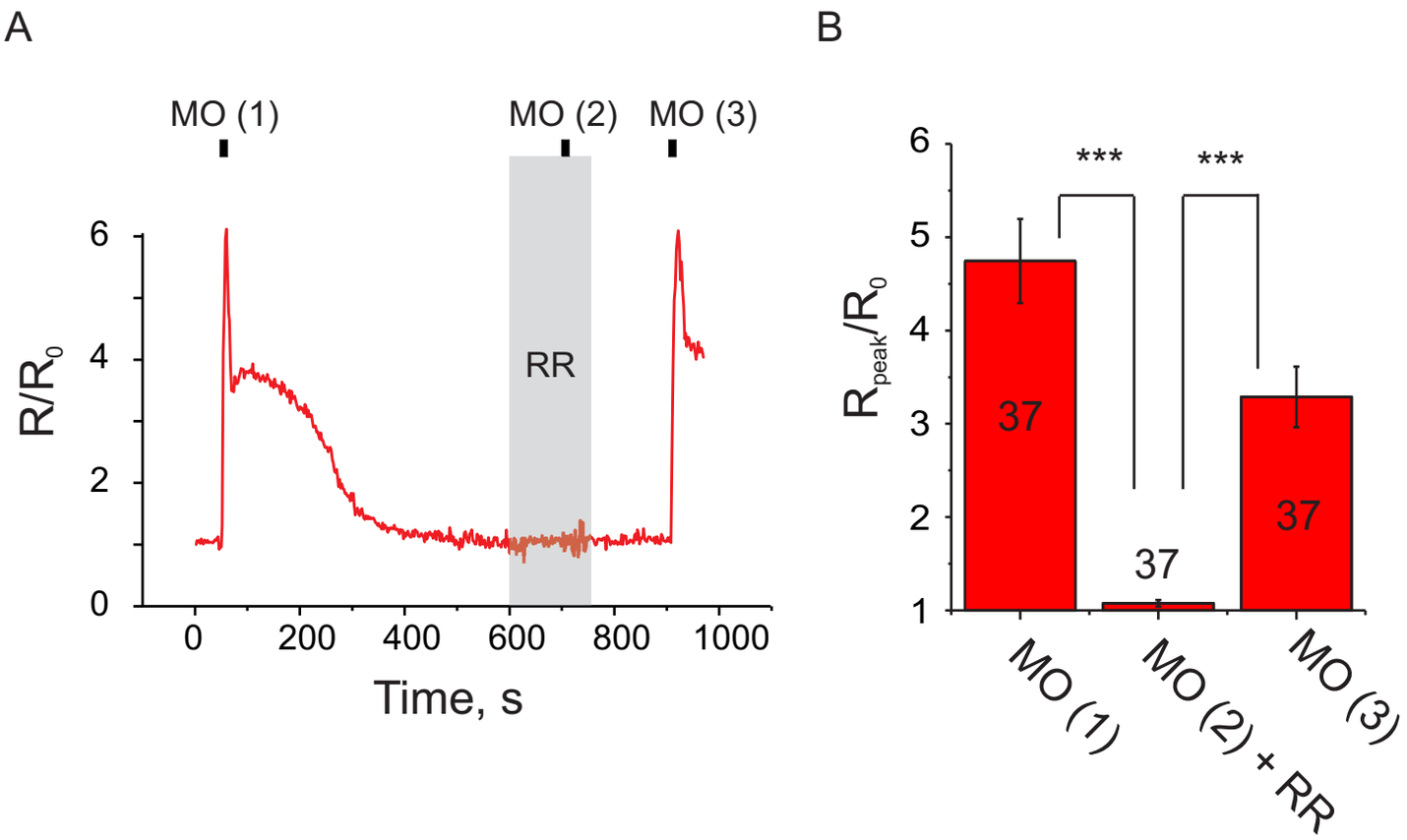

Supplementary Figure 6. Ruthenium red inhibits TRPA1 mediated Ca^{2+} influx in DRG neurons. TRPA1 was activated by bath application of mustard oil (MO) (100 μM) and cytosolic Ca^{2+} measured using fura-2. (A) Ruthenium red (RR) (10 μM) was added to the bath as indicated by the grey box. (B) Mean data following the protocol shown in A.

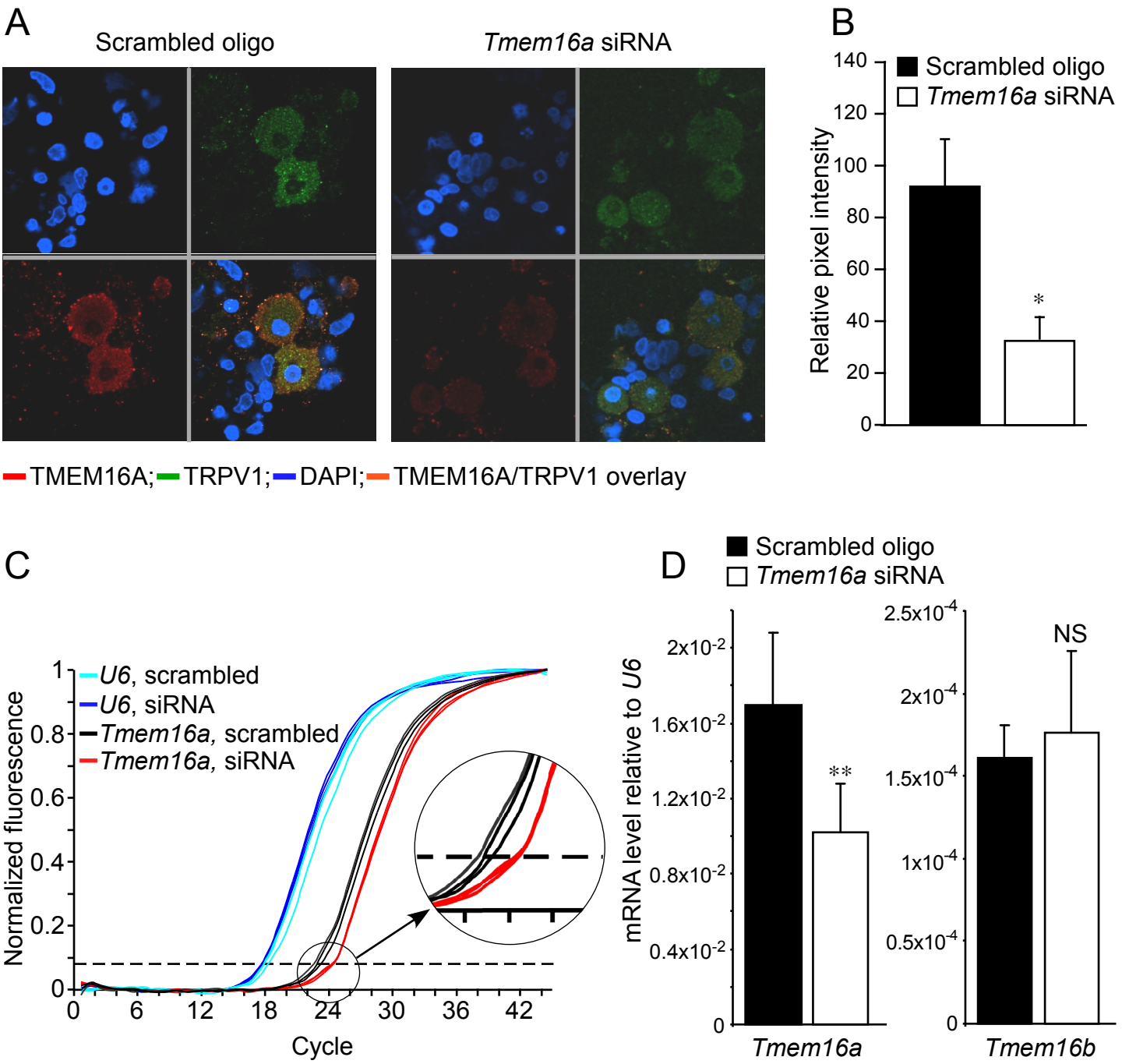

Supplementary Figure 7. Characterisation of *Tmem16a* siRNA knock-down. DRGs were extracted, dissociated and transfected with *Tmem16a* siRNA or scrambled oligonucleotides (control) using Amaxa Nucleofector device and cultured for 24 hours before harvest. (A) All TRPV1-positive neurons identified were TMEM16A-positive and anti-TMEM16A immunofluorescence was not identified in glia. Anti-TMEM16A single staining resulted in a similar immunofluorescence pattern. Control experiments that omitted anti-TMEM16A primary antibody did not result in immunofluorescence at the same settings (data not shown). (B) Quantification of pixel intensity for anti-TMEM16A immunofluorescence in TRPV1-positive neurons. TMEM16A staining was significantly reduced in *Tmem16a* siRNA transfected cells compared to control (n = 46 from 5 independent experiments; *p < 0.05 with two-tailed t-test). (C) Representative traces from quantitative reverse transcription-PCR showing triplicate results from one experiment. Each trace represents the increase in background-subtracted relative fluorescence per reaction in real time. Dotted line indicates threshold; increased threshold cycles for *Tmem16a* expression in siRNA versus control samples is magnified in the inset. (D) Mean relative mRNA levels from 6 independent experiments for *Tmem16a* (left) and 3 independent experiments for *Tmem16b* (right), normalized to the housekeeping gene *U6*, **p < 0.01. Each reaction was performed in triplicate. *Tmem16a* relative mRNA level was approximately 100 fold greater than *Tmem16b*.

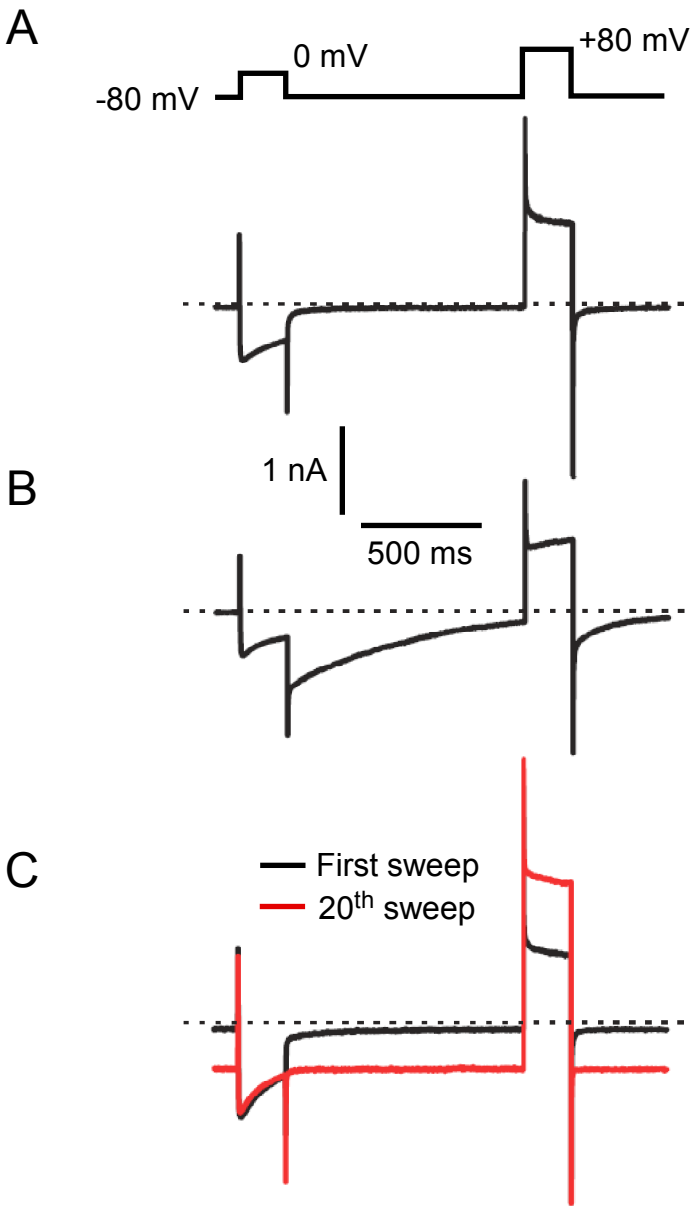

Supplementary Figure 8. Activation of Ca^{2+}-activated chloride current (CaCC) in DRG neurons by Ca^{2+} influx through the voltage-gated Ca^{2+} channels (VGCC). Voltage protocol is depicted above the current trace in A. (A) Majority of small capsaicin-positive DRG neurons (34/44) did not display measurable inward tail current following the activation of VGCC by the voltage step to 0 mV. In such cells tail current amplitudes after pulses to 0 mV (activation of VGCC, Ca^{2+} influx) and to +80 mV (activation of VGCC but no net Ca^{2+} influx due to the lack of driving force for Ca^{2+}) were similarly small (suggesting no CaCC activation). (B) 7/44 neurons displayed markedly higher tail currents elicited by the pulse to 0 mV as compared to the pulse to +80 mV suggesting activation of CaCC by Ca^{2+} influx. (C) 3/44 neurons displayed no or very little inward tail current after the first pulse to 0 mV but gradual development of a steady-state inward current following the repetitive application of voltage protocol. The inward currents shown on B and C were sensitive to 100 μM niflumic acid (not shown).

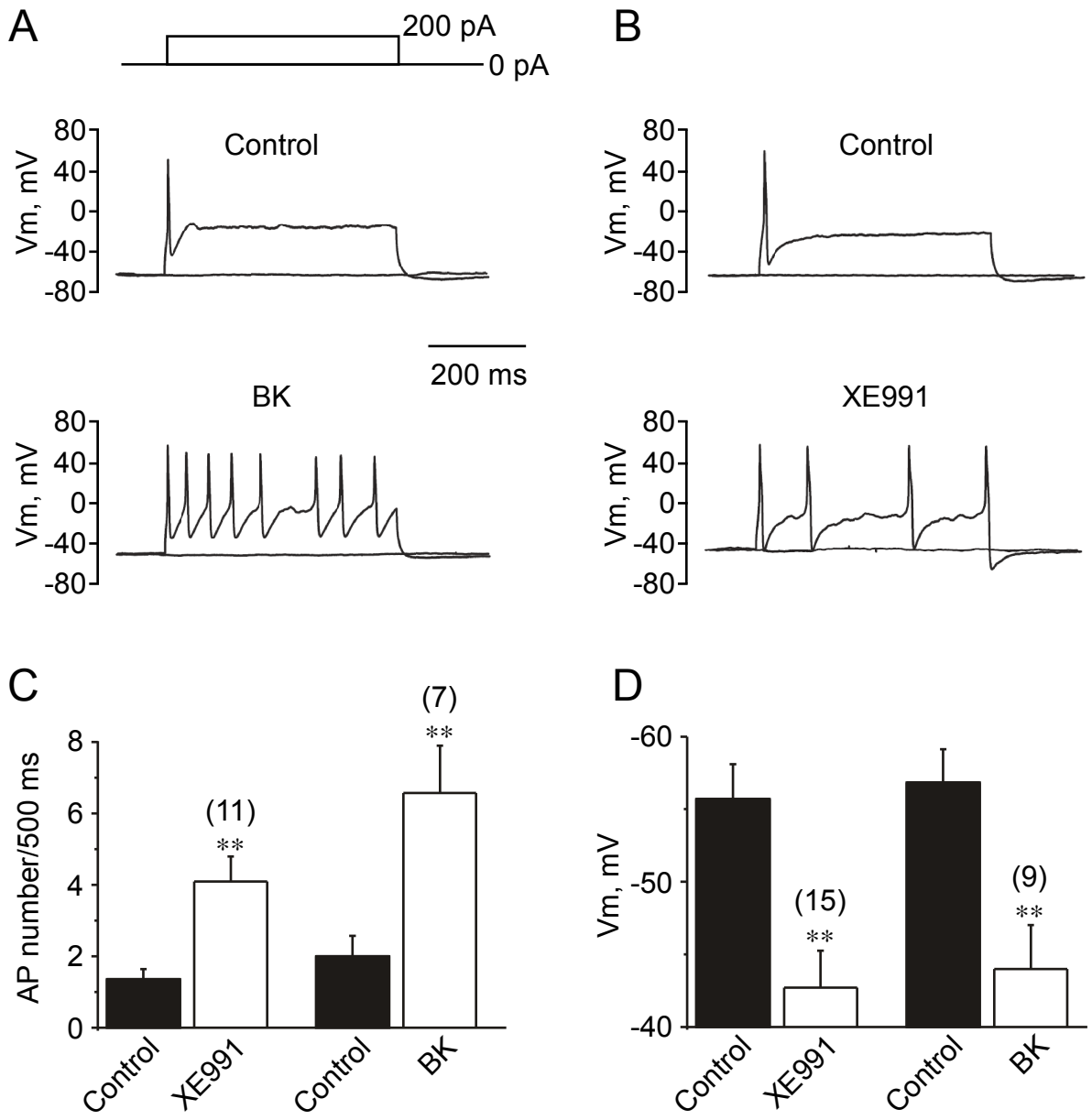

Supplementary Figure 9. Bradykinin and M channel blocker XE991 increase DRG neuron excitability. DRG neurons were studied under perforated-patch current clamp mode and action potentials were induced by a 500 ms injection of 200 pA current (as shown in the inset in A). (A) and (B) Effects of bradykinin (200 nM) and XE991 (3 μM) on the firing of action potentials in DRG neurons. The right panel shows the summary of the number of action potentials elicited in 500 ms duration. (C) is a summary of the effects shown on A and B. (D) depicts mean changes in resting membrane potential induced by BK or XE991; **p < 0.01.

Supplementary Methods

Preparation of purified DRG culture. DRG neurons were purified from non-neuronal cells by re-plating the culture 1 hour after the dissociation to remove adherent non-neuronal cells and culturing the enriched neuronal preparation in the presence of the antimitotic cytosine arabinoside (10 μM) for 48 hrs, after which medium was replaced with the normal growth medium and cells were cultured for another 3 days.

Quantitative RT-PCR, western blot. For real-time PCR, RNA was extracted using TRI reagent (Sigma) and 1 μg RNA added to the RT reaction. PCR was carried out in a MiIQ Single Colour Real-time PCR detection system (BioRAD) using gene specific primers. Western blot, TMEM16A (S-20) primary antibody (1:100, Santa Cruz), donkey anti-goat IgG-HRP secondary (1:1000, Sigma). Blot was stripped and reprobed with β-actin primary antibody (1:10000, Sigma), anti-mouse IgG-HRP secondary (1:1000, Sigma).

Immunocytochemistry. Cells were fixed in 3% paraformaldehyde and permeabilised with acetone:methanol (1:1) and labelled with anti-TRPV1 (Neuromics) and Alexa Fluor 488 donkey anti-guinea pig IgG (Molecular Probes); anti-TMEM16A (Santa Cruz) and Alexa Fluor 555 donkey anti-goat IgG (Molecular Probes); anti-Kv7.2 (gift from MS Shapiro, UTHSCSA, USA) and Alexa Fluor 633 donkey anti-rabbit IgG (Molecular Probes). DAPI staining was used to identify nuclei. Confocal images were taken with an LSM510 META microscope (Zeiss).

Electrophysiology. Recordings for the Supp. Fig. 8 were made in fast whole cell mode using extracellular solution containing (in mM) 130 tetraethylammonium chloride, 2 CaCl2, 1.5 MgCl2, 10 HEPES, and 10 glucose (pH 7.4 adjusted with CsOH). Pipette solution contained (in mM) 145 CsCl, 10 HEPES, 2 Mg-ATP, and 0.5 Na2-GTP (pH 7.35 adjusted with CsOH).